Pergamon

TETRAHEDRON

Tetrahedron 57 (2001) 6877–6883

A study on the effect of Lewis acid catalysis on the molecular mechanism of the cycloaddition between (*E*)-methyl cinnamate and cyclopentadiene

C. N. Alves,[a] F. F. Camilo,[b] J. Gruber[b] and A. B. F. da Silva[a,*]

[a]*Departamento de Química e Física Molecular, Instituto de Química de São Carlos, Universidade de São Paulo, CP 780, 13560-970 São Carlos, SP, Brazil*

[b]*Departamento de Química Fundamental, Instituto de Química, Universidade de São Paulo, CP 26077, 05513-970 São Paulo, SP, Brazil*

Received 13 November 2000; accepted 7 June 2001

Abstract—The molecular mechanism of the Diels–Alder reaction between (*E*)-methyl cinnamate and cyclopentadiene has been analyzed by means of AM1 semiempirical method and compared to the experimental results. Stationary points for two reactive channels, *endo-cis* and *exo-cis*, on potential energy surfaces have been characterized. Three Lewis acids, boron trifluoride (BF_3), aluminum trichloride ($AlCl_3$) and catechol boron bromide (CBB) have been used as catalysts taking into account the formation of a complex between the boron or aluminum atom and the carbonyl oxygen of (*E*)-methyl cinnamate. The molecular mechanism of the uncatalyzed reaction corresponds to a concerted process. In the presence of BF_3 and $AlCl_3$, enhancement of both the asynchronicity and charge transfer, with small decreased energy barriers, were obtained. With CBB, the molecular mechanism changes and the reaction takes place along a stepwise mechanism. The initial step corresponds to the nucleophilic attack of cyclopentadiene on the dienophile double bond to give an intermediate, followed by its closure in the second step, yielding the corresponding final cycloadduct. The inclusion of the CBB catalyst drastically decreases the energy barrier associated with the carbon–carbon bond formation of the first step, relative to the concerted process. The role of the Lewis acid catalyst emerges from the analysis of the results. © 2001 Elsevier Science Ltd. All rights reserved.

---

1. Introduction

The Diels–Alder (DA) reaction is one of the most widely used reactions in organic synthesis for obtaining cyclic systems. Lewis acid catalysts can have a significant effect on the rate and *endo* selectivity of DA reactions, especially when coordinated to a dienophile heteroatom, such as a carbonyl oxygen.[1,2]

This effect has also been the object of several theoretical studies[3–13] employing semiempirical methods,[3,4,13] ab initio[5–9,11] and density functional[10,12] which predict that the catalyst produces a notable increase in the asynchronicity of the transition states.

The reaction between cyclopentadiene and several *p*-substituted cinnamate esters and thioesters[14] in the presence and absence of some Lewis acids such as $Ti(OBu\text{-}n)_4$, $ZnCl_2$, $BF_3{\cdot}OEt_2$, $TiCl_4$, $AlCl_3$, BBr_3 and catechol boron bromide (CBB) has been investigated.[15–17] Surprisingly, only CBB led to all the desired adducts with very high yield. ^{13}C NMR chemical shifts of the dienophile carbonyl groups have shown a deshielding effect of approximately 4–7 ppm, after the addition of this catalyst, suggesting strong coordination. These experimental studies have offered the possibility to carry out a complementary theoretical analysis in order to attain a better interplay between theory and experiment.

This work presents an experimental and quantum chemical investigations of the effect of Lewis acid catalysis on the molecular mechanism of the DA reaction between (*E*)-methyl cinnamate (R1) and cyclopentadiene (CP). We performed a systematic AM1 semiempirical study through the localization of the stationary points: reactants, transition structure (TS), products and possible intermediates on the potential energy surface (PES) for this cycloaddition.

Our purpose in this work is to shed light on the mechanistic details of this important reaction. Lewis acid catalysts have been also included in order to clarify their role on the nature of the molecular mechanism.

2. Methods, computing procedures and models

Owing to the large size of the present systems, studies at the

---

Keywords: AM1 theoretical study; Diels–Alder reaction; Lewis acid catalyst; cycloaddition.

[*] Corresponding author. Fax: +55-16-2739975; e-mail: alberico@iqsc.sc.usp.br

PII: S0040-4020(01)00624-X

ab initio level are still a little bit expensive. However, semiempirical methods have progressed over the past few years to a surprising level of accuracy and reliability, considering the limitations of the underlying approximations.[18,19] Even simple calculations at moderate levels of theory such as semiempirical procedures give useful information on the molecular mechanism of different chemical reactions.

AM1[20] semiempirical calculations were carried out using the AMPAC 6.0[21] program. The PESs have been calculated in detail to ensure that all relevant stationary points have been located and properly characterized. Stationary points on PES were characterized by frequency calculations. The optimization was carried out by using the eigenvalue following routine[22] and the Berny analytical gradient optimization methods.[23,24] Finally, the nature of each stationary point was established by calculating analytically and diagonalizing the matrix of the energy second derivatives to determine the number of imaginary frequencies (zero for local minimum and one for a TS). The transition vector (TV),[25] i.e. the eigenvector associated to the unique negative eigenvalue of the force constant matrix has been characterized. The Intrinsic Reaction Coordinate (IRC) pathways from the TSs to the two lower energy structures have been traced using the second order Gonzalez and Schlegel interaction method[26,27] in order to verify that each saddle point links the two putative minima.

Four models have been selected for this study and the first one corresponds to the reaction between R1 and CP in the gas phase. The influence of the Lewis acid catalysts has been modeled taking into account the formation of a complex between the boron or aluminum atom and the carbonyl oxygen atom of R1 resulting in three more models: R1-BF_3 and CP, R1-$AlCl_3$ and CP and R1-CBB and CP.

As the dienophile, R1, can take two different conformations, *s-cis* or *s-trans*, which may bind with the diene, CP, to make a TS in two possible conformations, *endo* or *exo*, we have only considered in this work the *s-cis* approach, as the TSs *s-cis* and *s-trans* are rotamers.

At this point it is interesting to make a comment on the differences we have adopted in the geometry of the complexes in order to study the selected models (R1-BF_3 and CP, R1-$AlCl_3$ and CP and R1-CBB and CP). The reaction in the presence of CBB was the only one model involving the cation, as the other reactions were modeled with the neutral species. We did that based on the experimental results obtained from the ^{13}C NMR spectra of the dienophile and of the dienophile-CBB complex, where a downfield shift of 4 ppm (from 167 to 171 ppm, respectively) was observed for the carbonyl carbon, but in the BF_3 and $AlCl_3$ complexes no shift was observed.[15–17] The carbonyl carbon shift of 4 ppm in the CBB suggests a strong coordination, which is justified by a model without the Br atom, i.e. a cationic complex model. This is also the reason why we have adopted to model only the CBB reaction as trigonal rather than tetragonal, as we did for the other reactions.

3. Results and discussion

3.1. Experimental

(*E*)-Methyl cinnamate, aluminum chloride and boron trifluoride diethyl etherate were of commercial quality, reagent grade and used without further purification. Cyclopentadiene was prepared from its dimer, just before use. Boroncatechol bromide was obtained according to literature procedure[28] and used as a 0.2 mol L^{-1} solution in dichloromethane. All the solvents were dried and distilled before use. FT-IR spectra were recorded on a Perkin–Elmer 1750 series grating. Only major or important absorptions are given. ^{1}H NMR Fourier transform (FT) spectra were recorded on a Bruker AC-200 spectrometer using deuteriated chloroform/tetramethylsilane as solvent/reference. Column chromatography was performed utilizing silica gel, 70–230 mesh, 60 Å.

3.1.1. Procedures for the catalyzed DA reactions. *(a) In the presence of boroncatechol bromide*: to 12.5 mL (2.50 mmol) of a stirred 0.2 mol L^{-1} solution of boroncathecol bromide in dichloromethane at −22°C, under nitrogen atmosphere, a solution of (*E*)-methyl cinnamate (405 mg, 2.50 mmol) in dichloromethane (10.0 mL) was slowly added. After 30 min, a solution of freshly prepared cyclopentadiene (0.420 mL; 5.00 mmol) in dichloromethane (10.0 mL) was added dropwise and the mixture was stirred at −22°C for 5 h. The reaction was then quenched with water, extracted with dichloromethane, dried with $MgSO_4$, and concentrated. ^{1}H NMR spectrum of the crude product showed an *endo*/*exo* adduct ratio of 96:4. After purification by column chromatography (chloroform), 0.291 g (1.28 mmol, 51%) of *endo* 3-phenylbicyclo[2.2.1]hept-5-ene-2-carboxylic acid methyl ester was obtained as a viscous pale-yellow oil. IR (film) 3061 (CH), 2975 (CH), 1735 (C=O), 1601 (C=C), 1497 (C=C), 1435 (CH), 1311 (CH), 750 and 701 (CH) (lit.[29]: film, 1735 (C=O)); ^{1}H NMR δ 1.57 (d, 1H, J=8.7 Hz), 1.78 (d, 1H, J=8.7 Hz), 3.00 (dd, 1H, J=3.6, 5.0 Hz), 3.03 (m, 1H), 3.11 (dd, 1H, J=1.8, 5.0 Hz), 3.28 (m, 1H), 3.66 (s, 3H), 6.12 (dd, 1H, J=2.8, 5.6 Hz), 6.42 (dd, 1H, J=3.3, 5.6 Hz), 7.20–7.35 (m, 5H).

(b) In the presence of boron trifluoride diethyl etherate: the reaction was carried out as described above, except that the solvent was diethyl ether. The starting materials were fully recovered.

(c) In the presence of aluminum chloride: the reaction was carried out as described above, except that the solvent was benzene and the temperature was 25°C The starting materials were fully recovered.

3.2. Energies and geometries of stationary points

An exhaustive exploration of the PES for the formally [4+2] cycloaddition between R1 and CP affords that the reaction takes place through a concerted mechanism along two reactive channels corresponding to the *endo* and *exo*. Thus, we have found two TSs: TSen-R1 and TSex-R1 and two cycloadducts: Pen-R1 and Pex-R1, corresponding to the *endo* and *exo* approaches, respectively (see Table 1 and Fig.

Table 1. AM1 Relative energies (in kcal mol^{-1}) to reactants for the stationary points of the reactions between CP and R1, CP and R1-BF$_3$, CP and R1-AlCl$_3$ and CP and R1-CBB. Heats of formation (in kcal mol^{-1}) of the reactants in gas phase are: CP+R1=−10.98; CP+R1-BF$_3$=−290.70; CP+R1-AlCl$_3$=−154.18 and CP+R1-CBB=67.77

Models	Stationary points	Gas phase (kcal mol^{-1})	ΔE
R1+CP	Tsen	23.20	34.18
	Tsex	22.37	33.35
	Pen	−19.29	−8.31
	Pex	−19.82	−8.84
R1-BF$_3$+CP	TSen-BF$_3$	−257.53	33.17
	TSex-BF$_3$	−257.65	33.05
	Pen-BF$_3$	−301.16	−10.46
	Pex-BF$_3$	−302.17	−11.47
R1-AlCl$_3$+CP	TSen-AlCl$_3$	−120.07	34.11
	TSex-AlCl$_3$	−120.66	33.52
	Pen-AlCl$_3$	−161.69	−7.51
	Pex-AlCl$_3$	−162.40	−8.22
R1-CBB+CP	TS1en-CBB	82.23	14.57
	TS1ex-CBB	81.47	13.81
	INen-CBB	67.99	0.33
	INex-CBB	67.52	−0.14
	TS2en-CBB	77.96	10.30
	TS2ex-CBB	76.48	8.82
	Pen-CBB	60.58	−7.08
	Pex-CBB	60.21	−7.45

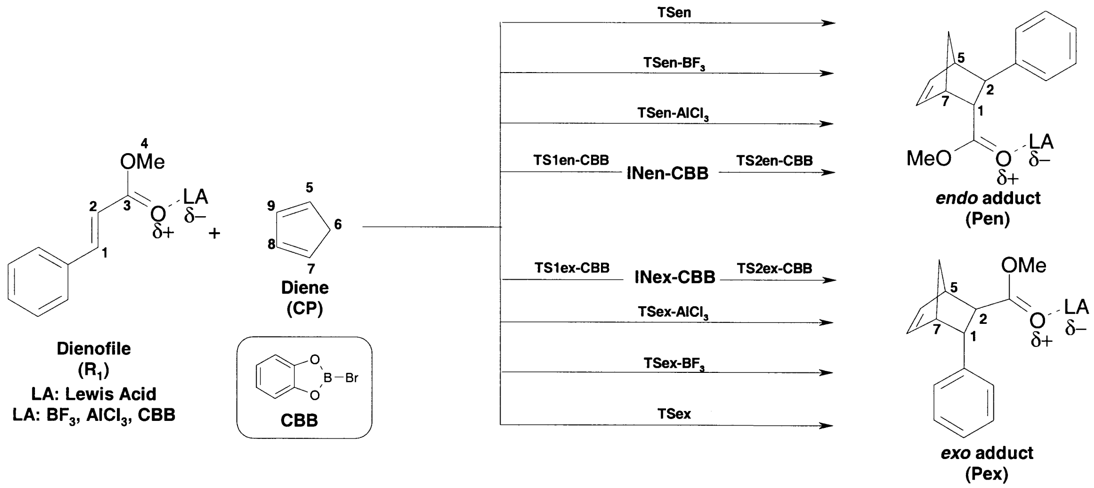

Figure 1. Representation of the uncatalyzed and catalyzed Diels–Alder reaction between (*E*)-methyl cinnamate (R1) and cyclopentadiene (CP).

1—the relative energies of the stationary points along the different reaction pathways are shown in Table 1). The barrier heights associated with these processes are: 34.18 and 33.35 kcal mol^{-1}, respectively, and formation of the cycloadducts are exothermic processes: −8.31 and −8.84 kcal mol^{-1}.

Semiempirical methods are known to have drawbacks when describing *endo*/*exo* selectivity. Cativiela et al.[30] have showed that conformational equilibra of the carbonyl-containing dienophiles and nonbonded interactions in the TS are poorly described both by AM1 and PM3 methods.

The TV is dominated by the motion forming the new C–C bonds and the extent of the asynchronicity (Δr) can be measured by means of the difference between the distances of the bonds that are being formed in the reaction, i.e. Δr: d(C2–C5)−d(C1–C7) at TSen-R1 or TSex-R1. The corresponding values are 0.03 and 0.02, respectively (see Table 2 and Fig. 2—the selected geometrical parameters of the different TSs are shown in Table 2). These results give a synchronous concerted mechanism.

The inclusion of BF$_3$ and AlCl$_3$ on R1 system led us to four TSs: TSen-BF$_3$ and TSex-BF$_3$, TSen-AlCl$_3$ and TSex-AlCl$_3$, and to four cycloadducts: Pen-BF$_3$ and Pex-BF$_3$, Pen-AlCl$_3$ and Pex-AlCl$_3$ corresponding to the *endo* and *exo* approaches, respectively (see Figs. 1 and 2). The barrier heights associated with these processes are: 33.17 and 33.05, 34.11 and 33.52 kcal mol^{-1}, respectively. Formations of the cycloadducts are exothermic processes: −10.46 and −11.47, −7.51 and −8.22 kcal mol^{-1}.

There is a small decrease of the energy barriers for TSen-BF$_3$, TSex-BF$_3$ and TSen-AlCl$_3$, 1.01, 0.30 and 0.07 kcal mol^{-1}, respectively, with respect to the uncatalyzed reactions and an increase of 0.17 kcal mol^{-1} for TSex-AlCl$_3$.

The large barrier height found for the three model reactions R1, R1-BF$_3$ and R1-AlCl$_3$+CP are in accordance with the

Table 2. Geometric parameters (distances in Å) and asynchronicity (Δr) for the TSs in vacuum for the reaction between CP and R1, CP and R1-BF_3, CP and R1-$AlCl_3$ and CP and R1-CBB

Models	Stationary points	C1–C7 (Å)	C2–C5 (Å)	O–B or O–Al (Å)	Δr
R1+CP	TSen-R1	2.098	2.130	–	0.032
	TSex-R1	2.106	2.127	–	0.021
R1-BF_3+CP	R1-BF_3	–	–	1.858	–
	TSen-BF_3	2.027	2.212	1.840	0.185
	TSex-BF_3	2.082	2.148	1.890	0.066
R1-$AlCl_3$+CP	R1-$AlCl_3$	–	–	1.823	–
	TSen-$AlCl_3$	1.937	2.240	1.812	0.303
	TSex-$AlCl_3$	1.974	2.353	1.798	0.379
R1-CBB+CP	R1-CBB	–	–	1.395	–
	TS1en-CBB	1.975	3.510	1.378	1.535
	TS1ex-CBB	1.966	3.577	1.377	1.611
	TS2en-CBB	1.568	2.296	1.383	0.728
	TS2ex-CBB	1.567	2.574	1.377	1.007

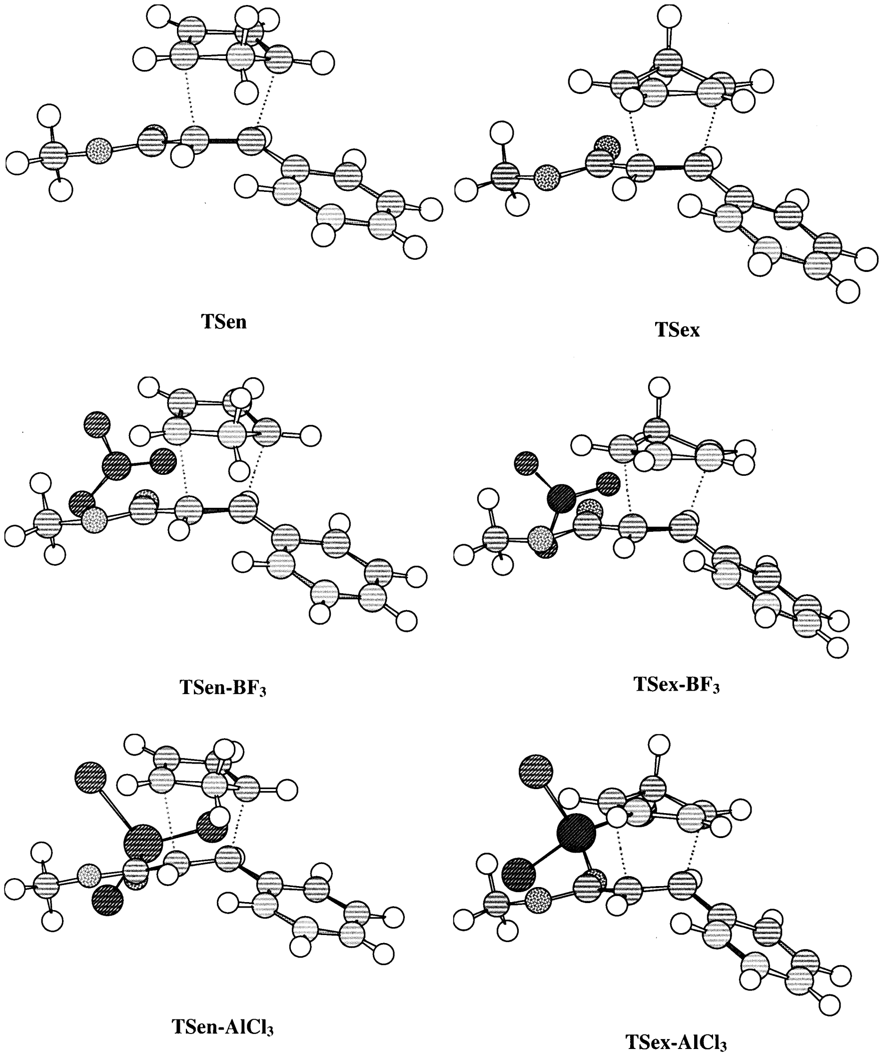
TSen **TSex**

TSen-BF_3 **TSex-BF_3**

TSen-$AlCl_3$ **TSex-$AlCl_3$**

Figure 2. Transition structures corresponding to the uncatalyzed and catalyzed reactions between CP and R1, R1-BF_3 and R1-$AlCl_3$.

experimental results, which show poor yield in the absence of a catalyst and no products at all in the presence of the catalysts.

As can be seen, the difference between the lengths of the two forming C–C bonds in the catalyzed process with BF_3 and $AlCl_3$ have increased, and consequently the transition states are more asynchronous than those of the uncatalyzed reaction (see Table 2 and Fig. 2). Similar result have already been observed in other catalyzed DA reactions[3–13] and can be attributed to a polarization of the antibonding π_{C-C} of the dienophile.[5–33]

With the Lewis acid CBB the cycloaddition most likely occurs through a stepwise mechanism. Four transition states and two intermediates have been found corresponding to the

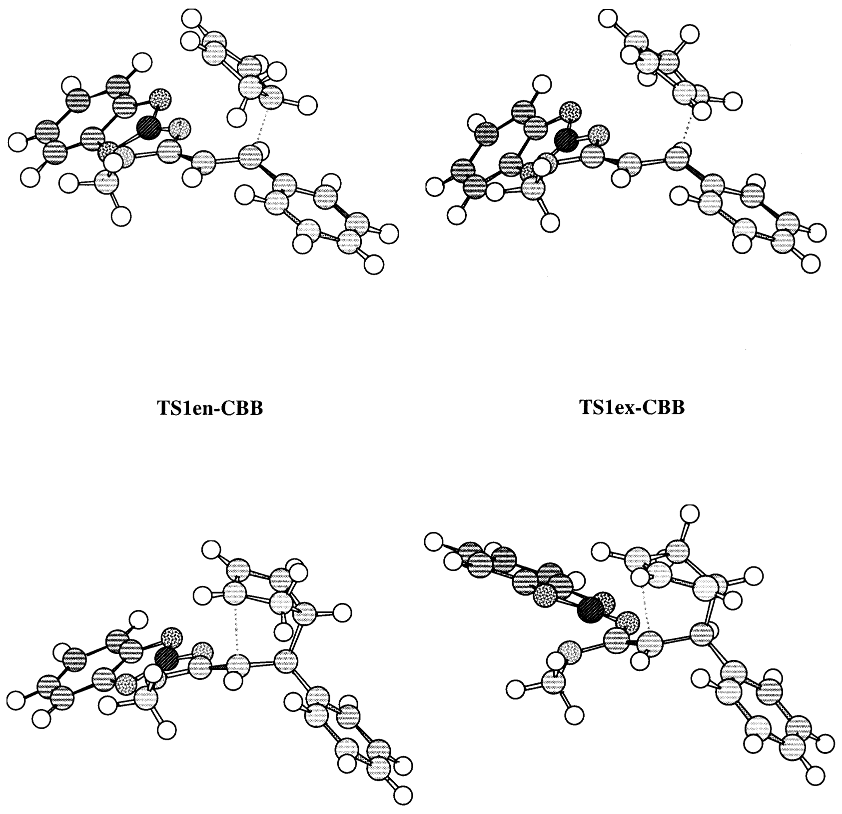

TS1en-CBB **TS1ex-CBB**

TS2en-CBB **TS2ex-CBB**

Figure 3. Transition structures corresponding to the catalyzed reactions between CP and R1-CBB.

endo and *exo* approaches of CP towards R1-CBB. For these catalyzed reactions, we have labeled the transition structures as TS1en-CBB, TS1ex-CBB, TS2en-CBB and TS2ex-CBB and the related minima corresponding to the final cycloadducts as Pen-CBB and Pex-CBB (see Figs. 1 and 3).

The first step of this formally [4+2] cycloaddition corresponds to the nucleophilic attack of the C7 carbon of CP to the C1 conjugated position of R1-CBB with formation of the corresponding intermediate (IN). The second step involves the ring-closure of these intermediates to give the final cycloadducts, achieved by the nucleophilic attack of the C2 position of R1-CBB to the allylic C5 position of the CP moiety. Inclusion of CBB drastically decreases the barrier height associated with the carbon–carbon bond formation in the first step related to the concerted process.

Table 3. Dipole moment (in Debye) and Mulliken population analysis of the charge transfer (in a.u.) for R1, R1-BF_3, R1-$AlCl_3$ and R1-CBB on the TSs for the Diels–Alder reaction between CP and R1, CP and R1-BF_3, CP and R1-$AlCl_3$ and CP and R1-CBB

Models	Stationary points	Dipole moment (Debye)	Q^T (a.u.)
R1+CP	Tsen	2.42	0.14
	Tsex	1.75	0.13
R1-BF_3+CP	TSen-BF_3	8.17	0.20
	TSex-BF_3	3.81	0.16
R1-$AlCl_3$+CP	TSen-$AlCl_3$	13.73	0.32
	TSex-$AlCl_3$	9.90	0.30
R1-CBB+CP	TS1en-CBB	6.86	0.44
	TS1ex-CBB	7.39	0.46
	TS2en-CBB	7.06	0.63
	TS2ex-CBB	9.05	0.74

The lengths of the C1–C7 forming bonds in the TSs of the first step are in the range of 1.966–1.975 Å while the distances between the C2 and C5 atoms are in the range of 3.510–3.577 Å. C2 and C5 atoms are not bonded during this step and only the C1–C7 bonds are formed due to the nucleophilic attack of CP to the β position of the coordinated unsaturated ester. In the intermediates, both C1 and C7 carbon atoms are completely pyramidalized and C8, C9 and C5 have a planar disposition in agreement with a sp^2 hybridization. This corresponds to an allylic arrangement for these three carbon atoms, which allows a favorable stabilization of the positive charge that is formed along the nucleophilic attack of CP to the unsaturated ester. The lengths of the C2–C5 forming bonds in the second TSs are in the range of 2.296–2.574 Å. The TVs of the first and second TSs are associated to C1–C7 and C2–C5 forming bonds, respectively.

The length of the B–O bond (1.39 Å) and the formation energy of the R1-CBB complex (−124.77 kcal mol^{-1}) are in accordance with the experimental results which show a strong complexation between the boron and the carbonyl oxygen atoms.[17] The geometries of all stationary points are available on request.

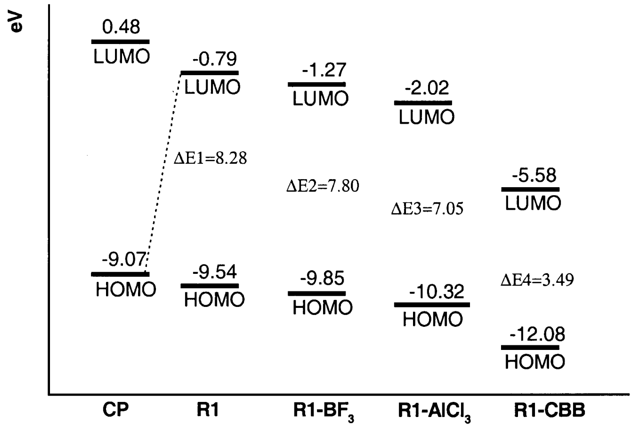

Figure 4. Energy of the frontier molecular orbitals for the cycloaddition reactions between CP and R1, R1-BF_3, R1-$AlCl_3$ and R1-CBB.

3.3. Mulliken population analysis

The Mulliken population analysis allowed us to analyze the charge transfer process along the reaction pathways of the cycloadditions. The low values found for the charge transfer at the TSs corresponding to the uncatalyzed process (around 0.1 a.u., see Table 3) are in agreement with a bond formation along the pericyclic process with a low polar character.

The charge transfers from CP to the R1-BF_3 and R1-$AlCl_3$ complexes in the transition structures are increased to 0.2 and 0.3 a.u., respectively, when compared to the uncatalyzed reactions. The charge transfers from CP to the unsaturated ester coordinated to CBB in the stepwise process are: 0.4 a.u. (first TSs), 0.6 a.u. (INs) and 0.7 a.u. (second TSs). These values indicate an increase of the charge transferred along the nucleophilic attack of CP to the electron-poor coordinated dienophile leading to the formation of the intermediates, since the cyclopentadiene fragment supports an appreciable positive charge. Therefore, the role of the Lewis acid catalyst can be understood as increasing the electrophilic character of the R1 system due to a stabilization of the corresponding TS through delocalization of the negative charge that is being transferred along the nucleophilic attack of CP. This fact is responsible for the change of the molecular mechanism in the catalyzed processes, which are accomplished by a lowering of the barrier heights. The uncatalyzed reaction, CP+R1, takes place along the pericyclic process with a larger value of the barrier height while the catalyzed reaction, CP+R1-CBB, corresponds to an ionic process initialized by the nucleophilic attack of CP to the unsaturated ester that is coordinated to the electron-poor Lewis acid. Therefore, CP and R1-CBB act as nucleophile and electrophile rather than a diene and dienophile, respectively.

From Tables 1–3 we can see that the increase of asynchronicity leads to an increase of charge transfer and, consequently, to a decrease of the energy barrier.

3.4. Frontier molecular orbital analysis

These reactions studied here can also be understood through the frontier molecular orbital (FMO) model, as the FMO model is capable of explaining the observed Lewis acid effects.[32] In Fig. 4, the role of the catalyst can be rationalized. For the uncatalyzed process, CP+R1, the main HOMO–LUMO interaction occurs between the HOMO of the diene ($HOMO_{CP}$) and the LUMO of the dienophile ($LUMO_{R1}$). $LUMO_{R1}$ presents high energy and this fact is consistent with the large barrier height found for the uncatalyzed process. However, when the boron or aluminum atoms are coordinated to the carbonyl oxygen of R1, the energies of both HOMO and LUMO of R1 decrease considerably. The reactivity order found was $\Delta E4=8.28$, $\Delta E3=7.80$, $\Delta E2=7.05$ and $\Delta E1=3.49$ eV. These calculations demonstrate that the frontier orbital energies are in qualitative agreement with both the energy barriers computed here and the experimental evidence.

4. Conclusions

In this work we have carried out an experimental and theoretical study on the effect of Lewis acid catalysis for the reaction between (*E*)-methyl cinnamate and cyclopentadiene. Reactions in the presence of BF_3, $AlCl_3$ and CBB acting as Lewis acids have been studied by using the AM1 semiempirical method. We stress that the present investigation concentrates on trends rather than absolute values. Although quantitative results are not expected with an AM1 semiempirical approach, general trends are reproduced and may help to elucidate the main factors responsible for the experimentaly observed outcomes. Inclusion of such factors is fundamental to a detailed understanding of chemical reactivity and they are desired before embarking on more elaborate theoretical treatments. Specific details of the global process may change at higher levels of theory (e.g. ab initio with correlation calculations), but despite the approximate procedure of the calculations employed here, some important features have been found.

The following conclusions can be drawn from the results obtained in this study: (a) cycloaddition between (*E*)-methyl cinnamate and cyclopentadiene takes place along a synchronous concerted mechanism. Two reactive channels have been characterized corresponding to the *endo*/*exo* approach modes; (b) in the presence of BF_3 and $AlCl_3$, enhancement of both the asynchronicity and the charge transfer were obtained with small decrease of the energy barriers; (c) coordination of the boron atom in the catechol boron bromide and the carbonyl oxygen atom in the (*E*)-methyl cinnamate changes the molecular mechanism from concerted to stepwise along two TSs and one intermediate (IN). The reaction mechanisms with BF_3 and $AlCl_3$ are fundamentally different than that in the presence of CBB. The calculations suggest that the Br must ionize from the intermediate to obtain reactivity. Also, the CBB reaction can be described as a nucleophilic attack of cyclopentadiene to the β position of the α,β-unsaturated ester with formation of the corresponding intermediate, followed by a ring closure process yielding the final cycloadduct. The AM1 semiempirical calculations with the CBB Lewis acid showed that the reaction pathway takes place with a very low barrier in a stepwise mechanism; (d) the present theoretical calculations identify the different factors controlling the reactive channels and the experimental outcome is reproduced.

Acknowledgements

The authors would like to thank CAPES, CNPq and FAPESP for their financial support.

References

1. Yates, P.; Eaton, P. *J. Am. Chem. Soc.* **1960**, *82*, 4436.
2. Inukai, T.; Kojima, T. *J. Org. Chem.* **1971**, *36*, 924.
3. Branchadell, V.; Oliva, A.; Bertrán, J. *J. Chem. Phys. Lett.* **1985**, *113*, 197.
4. Branchadell, V.; Oliva, A.; Bertrán, J. *J. Mol. Struct. (Theochem)* **1986**, *120*, 117.
5. Birney, D. M.; Houk, K. N. *J. Am. Chem. Soc.* **1990**, *112*, 4127.
6. González, J.; Houk, K. N. *J. Org. Chem.* **1992**, *57*, 3031.
7. Yamabe, S.; Daí, T.; Minato, T. *J. Am. Chem. Soc.* **1995**, *117*, 10994.
8. Daí, W. M.; Lau, C. W.; Chung, S. H.; Wu, Y. D. *J. Org. Chem.* **1995**, *60*, 8128.
9. Sbai, A.; Branchadell, V.; Ortunõ, R. M.; Oliva, A. *J. Org. Chem.* **1997**, *62*, 3049.
10. Garcia, J. I.; Martinez-Merino, V.; Mayoral, J. A.; Salvatella, L. *J. Am. Chem. Soc.* **1998**, *120*, 2415.
11. Dory, Y. L.; Hall, D. G.; Deslongchamps, P. *Tetrahedron* **1998**, *54*, 12279.
12. Alves, C. N.; Romero, O. A. S.; da Silva, A. B. F. *J. Mol. Struct. (Theochem)* **2001**, *535*, 165.
13. Alves, C.N.; da Silva, A.B.F.; Martí, S.; Moliner, V.; Oliva, M.; Andrés, J.; Domingo, L.R. *Tetrahedron*, submitted for publication.
14. Gruber, J.; Camilo, F. F. *J. Chem. Soc., Perkin Trans. 1* **1999**, 127.
15. Camilo, F. F.; Gruber, J. *Quím. Nova* **1999**, *22*, 382.
16. Zuckerman-Schpector, J.; Gruber, J.; Camilo, F. F. *Acta Crystallogr., Sect. C: Cryst. Struct. Commun.* **1999**, *55*, 980.
17. Camilo, F.F., MSc thesis, Instituto de Química, Universidade de São Paulo, Brazil 1998.
18. Stewart, J. J. P. *Semiempirical Molecular Orbitals Methods*, Wiley: New York, 1990.
19. Zerner, M. C. *Semiempirical Molecular Orbitals Methods*, Wiley: New York, 1991.
20. Dewar, M. J. S.; Zoebisch, E. G.; Healy, E. F.; Stewart, J. J. P. *J. Am. Chem. Soc.* **1995**, *107*, 3902.
21. AMPAC6.0. User's Manual; Semichem: Shawnee, 1997.
22. Baker, J. *J. Comput. Chem.* **1986**, *7*, 385.
23. Schlegel, H. B. *J. Chem. Phys.* **1982**, *77*, 3676.
24. Schlegel, H. B. *J. Comput. Chem.* **1982**, *3*, 214.
25. McIver, J. W. J. *Acc. Chem. Res.* **1974**, *7*, 72.
26. González, C.; Schlegel, H. B. *J. Phys. Chem.* **1990**, *94*, 5523.
27. González, C.; Schlegel, H. B. *J. Chem. Phys.* **1991**, *95*, 5853.
28. Stella, L.; Boucher, J. L. *Tetrahedron Lett.* **1982**, *23*, 953.
29. Nicolas, L.; Beugelmans-Verrier, M.; Guilhem, J. *Tetrahedron* **1981**, *37*, 3848.
30. Cativiela, C.; Dillet, V.; García, J. I.; Mayoral, J. A.; Ruiz-López, M. F.; Salvatella, L. *J. Mol. Struct. (Theochem)* **1995**, *331*, 37.
31. Houk, K. N.; Strozier, R. W. *J. Am. Chem. Soc.* **1973**, *95*, 4094.
32. Fleming, I. *Frontier Orbitals and Organic Chemical Reactions*, Wiley: New York, 1996.
33. Guner, O. F.; Strozier, R. M. *J. Am. Chem. Soc.* **1987**, *52*, 391.